Monotonization of a Family of Implicit Schemes for the Burgers Equation

Alexander Kurganov and Petr N. Vabishchevich

Abstract We study numerical methods for convection-dominated fluid dynamics problems. In particular, we consider initial-boundary value problems for the Burgers equation with small diffusion coefficients. Our goal is to investigate several strategies, which can be used to monotonize numerical methods and to ensure non-oscillatory and positivity-preserving properties of the computed solutions. We focus on fully implicit finite-element methods constructed using the backward Euler time discretization combined with high-order spatial approximations. We experimentally study the following three monotonization approaches: mesh refinement, increasing the time-step size and utilizing higher-order finite-element approximations. Feasibility of these three strategies is demonstrated on a number of numerical examples for both one- and two-dimensional Burgers equations.

1 Introduction

We study numerical methods for convection-dominated nonlinear convection-diffusion equations; see, e.g., [2, 21, 25, 29].

In practice, it is often important to design numerical methods that produce monotone, non-oscillatory and positivity-preserving computed solutions. This has been done for both linear and nonlinear convective terms; see, e.g., [12, 14, 16] and references therein.

A classical approach in enforcing monotonicity of computed solutions of hyperbolic and convection-dominated problems is by introducing artificial viscosity. The

Alexander Kurganov
Department of Mathematics, Southern University of Science and Technology, Shenzhen, 518055, China e-mail: alexander@sustech.edu.cn

Petr N. Vabishchevich
Nuclear Safety Institute of the Russian Academy of Sciences, 115191, Moscow, Russia and North-Eastern Federal University, 677000, Yakutsk, Russia, e-mail: vabishchevich@gmail.com

concept of artificial viscosity was first introduced back in 1950 in [28]. For modern artificial viscosity methods we refer the reader to, e.g., [8, 9, 15]. Non-oscillatory and positivity-preserving properties can be also ensured by using upwind approximations and nonlinear limiters; see, e.g., [7, 10, 13, 18] and references therein.

In this paper, we investigate several strategies, which can be used to suppress spurious oscillations in the computed solutions of the initial-boundary value problems (IBVPs) for the Burgers equation without adding artificial viscosity or utilizing any special approximations of the convection term.

We implement standard finite-element spatial approximations [6, 17], which are widely used in computational fluid dynamics [5,30]. One of the key points in designing a non-oscillatory numerical method is choosing an appropriate time discretization. When numerically solving IBVPs for linear convection-diffusion equations, two-level schemes (θ-method, schemes with weights) are traditionally widely used; see, e.g., [3, 19]. For these methods, the monotonicity of the computed solution is studied using the discrete maximum principle; see, e.g., [23, 24]. We would like to point out that even in the simplest purely diffusive case, the only unconditionally monotone scheme is the fully implicit backward Euler one. Other two-level schemes are only conditionally monotone with the monotonicity restriction on the time-step size τ being very strict, namely, $\tau = \mathcal{O}(h^2)$, where h is the spatial mesh size. We therefore use only the fully implicit backward Euler method in the current study. We implement the implicit scheme with the help of the classical iterative Newton's method [22], which is used to obtain the solution at the new time level. Alternative approaches for the realization of the implicit schemes are discussed in [11].

The main goal of this paper is to investigate the following three monotonization strategies. The first one is reducing the spatial mesh size. This approach would lead to a monotone positivity-preserving numerical solution provided h is taken to be proportional to the diffusion coefficient. Such restriction, however, may become impractical for multidimensional problems with small diffusion. The second strategy is increasing the time-step size. By doing this we take advantage of the fact that the use of the backward Euler temporal discretization introduces a numerical diffusion proportional to τ. The numerical effect of this type of monotonization has been recently demonstrated in [27], where a simple implicit finite-element method for isentropic gas dynamics equations has been proposed. The third strategy is increasing the order (p) of the spatial finite-element approximation. As it has been demonstrated in [4], this helps to suppress the oscillations in computed solutions of stationary convection-diffusion equations.

In this paper, we experimentally study the three aforementioned monotonization strategies in the context of nonlinear convection-diffusion equations in the convection-dominated regime. To this end, we vary the parameters h, τ and p and verify that reducing the spatial mesh or time-step size or increasing the order of spatial approximation help to obtain non-oscillatory, positivity-preserving numerical solutions.

The paper is organized as follows. In §2, we formulate the studied IBVP for the one-dimensional (1-D) Burgers equation and the family of implicit finite-element methods for its numerical solution. In §3, we conduct the aforementioned experi-

mental monotonization study for the 1-D IBVP. In §4, we extend our study to the IBVP for the two-dimensional (2-D) Burgers equation. Some concluding remarks on efficiency and accuracy of the resulting method are given in §5.

2 One-Dimensional Problem

We consider the 1-D Burgers equation,

$$u_t + \Big(\frac{u^2}{2}\Big)_x = \nu u_{xx}, \quad x \in \Omega = (-1,1), \quad t \in (0,T], \tag{1}$$

where $\nu > 0$ is a constant diffusion coefficient, subject to the following initial and boundary conditions:

$$u(x,0) = u_0(x), \quad x \in \Omega, \tag{2}$$

$$u_x(-1,t) = u_x(1,t) = 0, \quad t \in (0,T]. \tag{3}$$

We design the numerical method for the IBVP (1)–(3) based on the finite-element spatial approximations; see, e.g., [26]. For the sake of simplicity, we will use a uniform grid with the nodes $x_j = jh,\ j = 0,\dots,M,\ Mh = |\Omega| = 2$.

We define the finite-element space $V^h \subset H^1(\Omega)$ and approximate the solution on each finite element using polynomials of degree p. The approximate solution $\psi \in V^h$ is then obtained from the following two integral equations:

$$\int_\Omega \psi_t v\,\mathrm{d}x + \int_\Omega \Big(\frac{\psi^2}{2}\Big)_x v\,\mathrm{d}x + \nu \int_\Omega \psi_x v_x\,\mathrm{d}x = 0, \quad t \in (0,T], \tag{4}$$

$$\int_\Omega \psi(x,0)v(x)\,\mathrm{d}x = \int_\Omega u_0(x)v(x)\,\mathrm{d}x, \tag{5}$$

which should be satisfied for all $v \in V^h$.

Let τ be a uniform time-step size and denote by $\psi^n(x) := \psi(x,t^n)$, where $t^n := n\tau,\ n = 0,\dots,N,\ N\tau = T$. In order to numerically solve the problem (4), (5), we use fully implicit scheme, which results in the following integral equation:

$$\int_\Omega \frac{\psi^{n+1}-\psi^n}{\tau} v\,\mathrm{d}x + \int_\Omega \Big(\frac{(\psi^{n+1})^2}{2}\Big)_x v\,\mathrm{d}x + \nu \int_\Omega \psi_x^{n+1} v_x\,\mathrm{d}x = 0, \quad n = 0,\dots,N-1, \tag{6}$$

subject to the corresponding initial condition:

$$\int_\Omega \psi^0 v\,\mathrm{d}x = \int_\Omega u_0 v\,\mathrm{d}x. \tag{7}$$

In order to solve the nonlinear variational problem (6), (7), the iterative Newton method is applied [22]. The computational implementation is based on the FEniCS platform for solving partial differential equations [1, 20]. A standard convergence/stopping criterion has been used for the iterative process. Calculations finished when both the absolute and relative (with respect to the initial value) residuals become smaller than the prescribed tolerances. In the numerical experiments reported below, we take the tolerances 10^{-9} for the absolute residual and 10^{-8} for the relative one.

3 Numerical Monotonization

We consider a particular example of the 1-D Burgers equation (1) with different values of ν subject to the following initial condition:

$$u_0(x) = \begin{cases} 1+\cos(2\pi(x+0.5)), & -1 \le x < 0, \\ 0, & 0 \le x \le 1. \end{cases} \tag{8}$$

We note that the exact solution of the IBVP (1), (8), (3) is bounded and

$$0 \le u(x,t) \le u_{\max}, \quad u_{\max} := \max_{-1\le x\le 1} u_0(x) = 2.$$

We will compare the computed solutions below with the corresponding reference solutions, which are obtained on a very fine mesh with $M = 50000$ using the piecewise-linear finite elements ($p = 1$) and the time-step size τ selected based on the CFL condition with the CFL number equal to 1, namely:

$$\tau = \tau_0 := \frac{h}{u_{\max}} = \frac{1}{M}. \tag{9}$$

The reference solutions at the final time $T = 1$ are plotted in Figure 1 (left) for $\nu = 10^{-2}, 10^{-3}, 10^{-4}$ and 10^{-5}. Zoom at the shock area is shown in Figure 1 (right).

We now turn to the study of the three aforementioned monotonization strategies.

3.1 Spatial Mesh Refinement

We compute the solutions of the IBVP (1), (8), (3) with $\nu = 10^{-2}$, 10^{-3}, 10^{-4} and 10^{-5} and present the obtained results in Figure 2 for three different meshes with $M = 100$, 400 and 1600 and the time-step size selected based on the CFL condition (9). As one can clearly see, when $\nu = 10^{-2}$, all of the three computed solutions are monotone and non-negative. This is, however, not true for $\nu = 10^{-3}$, for which mesh refinement is required since the solution computed on the coarse

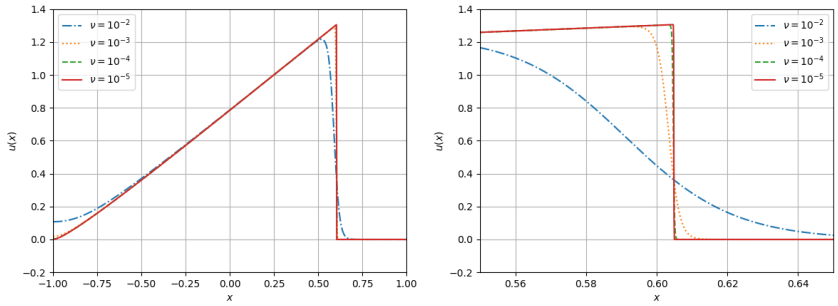

Fig. 1 Reference solutions for different values of ν (left) and zoom at the shock area (right).

grid with $M = 100$ is oscillatory. For the smaller values of $\nu = 10^{-4}$ and 10^{-5}, all of the three computed solutions are oscillatory and one needs to further refine the mesh to suppress these oscillations. One can, however, observe that the area where the oscillations are spread shrinks as M increases. We also note that in the case of $\nu = 10^{-4}$, the amplitude of oscillations reduces when the mesh is refined.

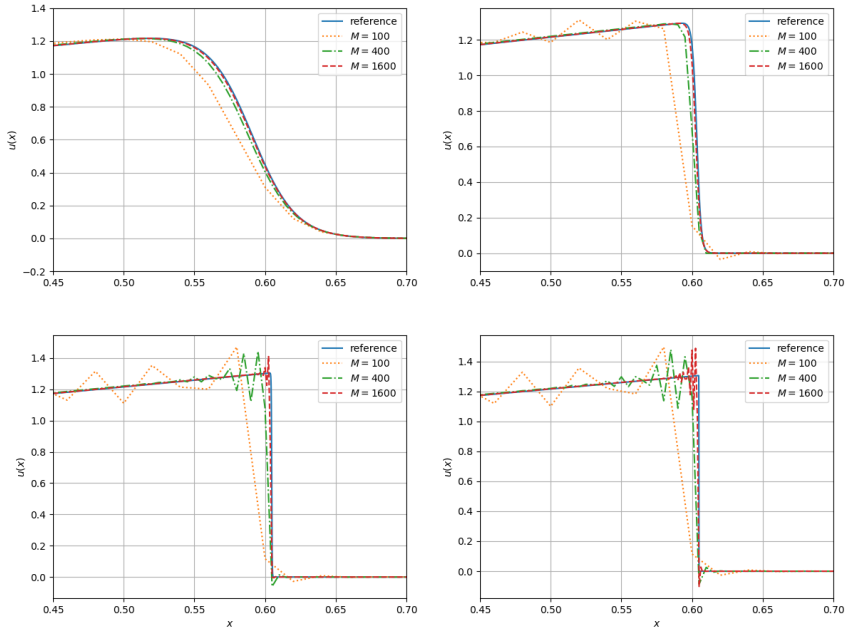

Fig. 2 Computed (with $M = 100$, 400 and 1600) and reference solutions for $\nu = 10^{-2}$ (top left), $\nu = 10^{-3}$ (top right), $\nu = 10^{-4}$ (bottom left) and $\nu = 10^{-5}$ (bottom right).

3.2 Enlarging Time-Step Size

Once again, we compute the solutions of the IBVP (1), (8), (3) with $\nu = 10^{-2}$, 10^{-3}, 10^{-4} and 10^{-5}. We now fix $M = 400$ and set $\tau = \gamma\tau_0$ with three different values of $\gamma = 1$, 2 and 4. The obtained results are presented in Figure 3, where one can clearly see the smoothing effect of time-step enlargement. In particular, we emphasize that even for smaller diffusion coefficients $\nu = 10^{-4}$ and 10^{-5}, the solutions computed with the largest time-step size, that is, with $\gamma = 4$ are oscillation-free and positive.

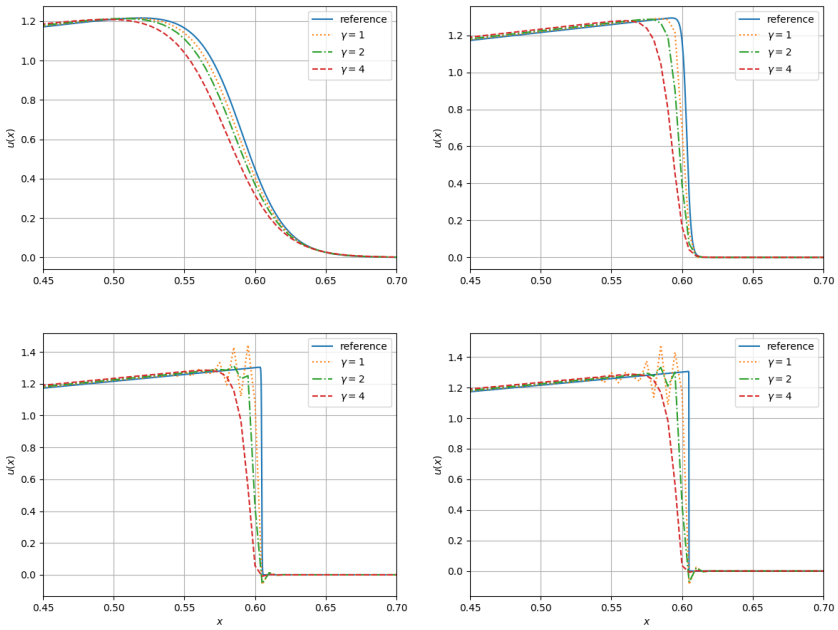

Fig. 3 Computed (with $M = 400$ and $\tau = \gamma\tau_0$ with $\gamma = 1$, 2 and 4) and reference solutions for $\nu = 10^{-2}$ (top left), $\nu = 10^{-3}$ (top right), $\nu = 10^{-4}$ (bottom left) and $\nu = 10^{-5}$ (bottom right).

3.3 Increasing the Order of Spatial Approximation

Finally, we compute the solutions of the IBVP (1), (8), (3) with $\nu = 10^{-2}$, 10^{-3}, 10^{-4} and 10^{-5} using the Lagrangian finite elements of orders $p = 1$, 2 and 4 on the fixed mesh with $M = 200$ and τ determined by the CFL condition (9). The obtained results are plotted in Figure 4. As one can observe, in the case of large diffusion coefficient $\nu = 10^{-2}$, the computed solutions are almost identical; when $\nu = 10^{-3}$,

the solution obtained with $p = 1$ is oscillatory, while the solutions computed with $p = 2$ and 4, which are very close to each other, are non-oscillatory and positive; when $\nu = 10^{-4}$ and 10^{-5}, the oscillations are still suppressed by the use of higher-order finite elements and the solution computed with $p = 4$ is clearly sharper than the one obtained with $p = 2$.

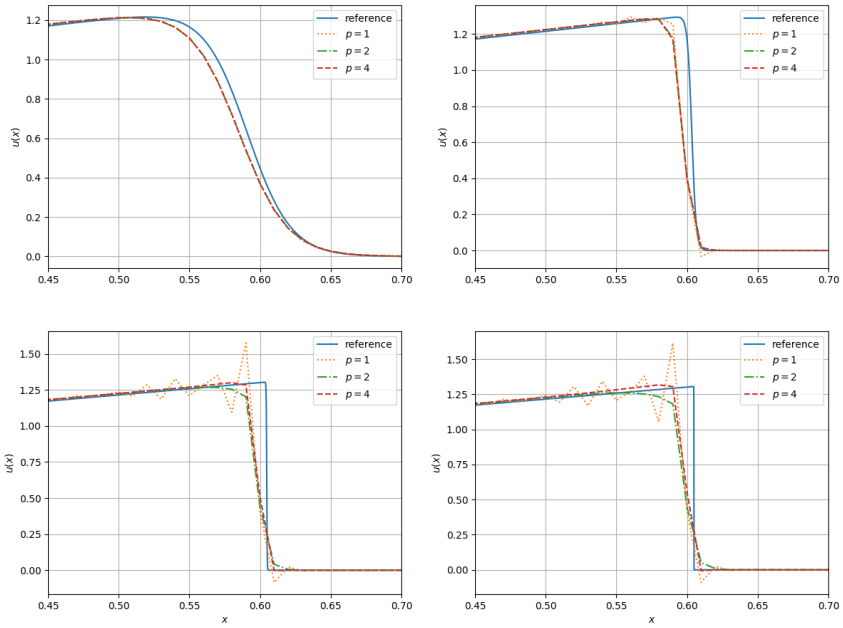

Fig. 4 Computed (with $M = 200$, $\tau = \tau_0$ and $p = 1$, 2 and 4) and reference solutions for $\nu = 10^{-2}$ (top left), $\nu = 10^{-3}$ (top right), $\nu = 10^{-4}$ (bottom left) and $\nu = 10^{-5}$ (bottom right).

4 Two-Dimensional Problem

In this section, we consider the 2-D Burgers equation,

$$u_t + \left(\frac{u^2}{2}\right)_x + \left(\frac{u^2}{2}\right)_y = \nu(u_{xx} + u_{yy}), \quad (x,y) \in \Omega = (-1,1) \times (-1,1), \quad t \in (0,T], \tag{10}$$

where $\nu > 0$ is, as before, a constant diffusion coefficient. The initial and boundary conditions are

$$u(x,y,0) = u_0(x,y), \quad (x,y) \in \Omega, \tag{11}$$

$$u_x(-1,y,t) = u_x(1,y,t) = u_y(x,-1,t) = u_y(x,1,t) = 0, \quad t \in (0,T]. \tag{12}$$

We consider a particular example of the 2-D Burgers equation (1) with $\nu = 10^{-4}$ subject to the following initial condition:

$$u_0(x,y) = 2e^{-10\left((x+0.5)^2+(y+0.5)^2\right)}. \tag{13}$$

We note that as in the 1-D example studied in §3, the exact solution of the IBVP (10)–(13) is bounded and $0 \le u(x,y,t) \le u_{\max} := \max_{(x,y)\in\Omega} u_0(x,y) = 2$.

We numerically solve the IBVP (10)–(13) using a family of implicit finite-element methods with $p = 1$, 2 and 4 on a uniform $M \times M$ Cartesian mesh with $M = 200$ and the time-step size taken according to the CFL condition with the CFL number equal to 1, namely: $\tau = (2/M)/u_{\max} = 1/M$. The solutions computed at the final time $T = 1$ are shown in Figure 5. As one can see, when $p = 1$ is used, the obtained solution is quite oscillatory. The oscillations are, however, substantially decreased by using $p = 2$ and almost eliminated when $p = 4$.

5 Concluding Remarks

In this paper, we have experimentally studied three monotonization strategies in the context of nonlinear convection-diffusion equations in the convection-dominated regime. We have varied the spatial mesh size (h), time-step (τ) and spatial formal order of the method (p) and verified that reducing h, increasing τ or increasing p helps to obtain non-oscillatory, positivity-preserving numerical solutions. Obviously, when h is reduced or p is increased, the CPU time will increase, which may affect the efficiency of the method. On the other hand, whet τ is increased, the accuracy of the method is affected. We therefore suggest the author to mix the studied strategies in order to obtain an accurate, non-oscillatory and efficient resulting method. Details of the optimal strategy depends on problem at hand and also on the computational resources available.

Acknowledgements The work of A. Kurganov was supported in part by NSFC grant 11771201. The work of P. N. Vabishchevich was supported in part by Russian Federation Government mega-grant 14.Y26.31.0013. The authors would like to thank anonymous reviewers for their valuable suggestions and corrections.

References

1. Alnæs, M., Blechta, J., Hake, J., Johansson, A., Kehlet, B., Logg, A., Richardson, C., Ring, J., Rognes, M.E., Wells, G.N.: The FEniCS project version 1.5. Archive of Numerical Software **3**(100), 9–23 (2015)

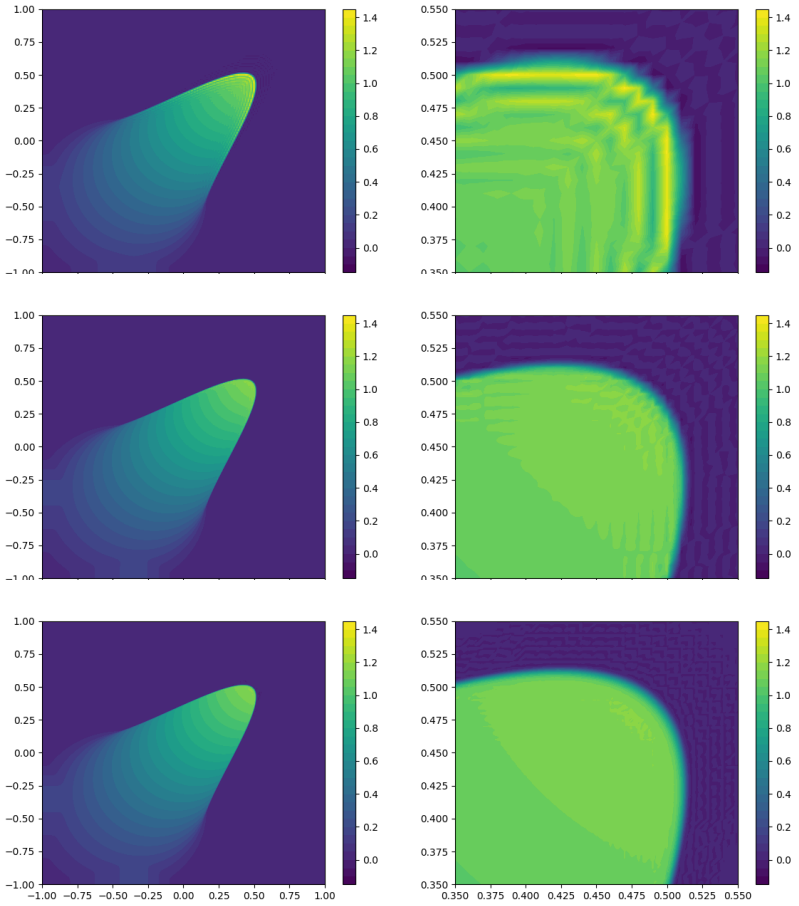

Fig. 5 2-D solutions computed using $p = 1$ (top row), 2 (middle row) and 4 (bottom row). The solutions are plotted in the entire Ω (left column) and zoomed at the shock front area (right column).

2. Anderson, J.D.: Computational Fluid Dynamics: The Basics with Applications. Mechanical engineering series. McGraw-Hill, New York, NY (1995)
3. Ascher, U.M.: Numerical Methods for Evolutionary Differential Equations, *Computational Science & Engineering*, vol. 5. Society for Industrial and Applied Mathematics (SIAM), Philadelphia, PA (2008)
4. Cai, Q., Kollmannsberger, S., Sala-Lardies, E., Huerta, A., Rank, E.: On the natural stabilization of convection dominated problems using high order Bubnov-Galerkin finite elements. Comput. Math. Appl. **66**(12), 2545–2558 (2014)
5. Donea, J., Huerta, A.: Finite Element Methods for Flow Problems. Wiley (2003)
6. Ern, A., Guermond, J.L.: Theory and Practice of Finite Elements, *Applied Mathematical Sciences*, vol. 159. Springer-Verlag, New York (2004)

7. Godlewski, E., Raviart, P.A.: Numerical Approximation of Hyperbolic Systems of Conservation Laws, *Applied Mathematical Sciences*, vol. 118. Springer-Verlag, New York (1996)
8. Guermond, J.L., Pasquetti, R., Popov, B.: Entropy viscosity method for nonlinear conservation laws. J. Comput. Phys. **230**(11), 4248–4267 (2011)
9. Hartmann, R., Houston, P.: Adaptive discontinuous Galerkin finite element methods for nonlinear hyperbolic conservation laws. SIAM J. Sci. Comput. **24**(3), 979–1004 (2002)
10. Hesthaven, J.S.: Numerical Methods for Conservation Laws, *Computational Science & Engineering*, vol. 18. Society for Industrial and Applied Mathematics (SIAM), Philadelphia, PA (2018). From analysis to algorithms
11. van der Houwen, P.J., Sommeijer, B.P., Kok, J.: The iterative solution of fully implicit discretizations of three-dimensional transport models. Appl. Numer. Math. **25**(2-3), 243–256 (1997). Special issue on time integration (Amsterdam, 1996)
12. Hundsdorfer, W., Verwer, J.: Numerical solution of time-dependent advection-diffusion-reaction equations, *Springer Series in Computational Mathematics*, vol. 33. Springer-Verlag, Berlin (2003)
13. Kröner, D.: Numerical Schemes for Conservation Laws. Wiley-Teubner Series Advances in Numerical Mathematics. John Wiley & Sons Ltd., Chichester (1997)
14. Kulikovskii, A.G., Pogorelov, N.V., Semenov, A.Y.: Mathematical Aspects of Numerical Solution of Hyperbolic Systems, *Chapman & Hall/CRC Monographs and Surveys in Pure and Applied Mathematics*, vol. 118. Chapman & Hall/CRC, Boca Raton, FL (2001)
15. Kurganov, A., Liu, Y.: New adaptive artificial viscosity method for hyperbolic systems of conservation laws. J. Comput. Phys. **231**, 8114–8132 (2012)
16. Kuzmin, D.: A Guide to Numerical Methods for Transport Equations. University Erlangen-Nuremberg (2010)
17. Larson, M.G., Bengzon, F.: The Finite Element Method: Theory, Implementation, and Applications, *Texts in Computational Science and Engineering*, vol. 10. Springer, Heidelberg (2013)
18. LeVeque, R.J.: Finite Volume Methods for Hyperbolic Problems. Cambridge Texts in Applied Mathematics. Cambridge University Press, Cambridge (2002)
19. LeVeque, R.J.: Finite Difference Methods for Ordinary and Partial Differential Equations. Society for Industrial and Applied Mathematics (SIAM), Philadelphia, PA (2007). Steady-State and Time-Dependent Problems
20. Logg, A., Mardal, K.A., Wells, G.: Automated Solution of Differential Equations by the Finite Element Method: The FEniCS Book, vol. 84. Springer Science & Business Media (2012)
21. Morton, K.W.: Numerical Solution of Convection-Diffusion Problems, *Applied Mathematics and Mathematical Computation*, vol. 12. Chapman & Hall, London (1996)
22. Ortega, J.M., Rheinboldt, W.C.: Iterative Solution of Nonlinear Equations in Several Variables, *Classics in Applied Mathematics*, vol. 30. Society for Industrial and Applied Mathematics (SIAM), Philadelphia, PA (2000). Reprint of the 1970 original
23. Samarskii, A.A.: The Theory of Difference Schemes, *Monographs and Textbooks in Pure and Applied Mathematics*, vol. 240. Marcel Dekker, Inc., New York (2001)
24. Samarskii, A.A., Gulin, A.V.: Ustoĭchivost' Raznostnykh Skhem (Russian) [Stability of Difference Schemes], second edn. Editorial URSS, Moscow (2004)
25. Samarskii, A.A., Vabishchevich, P.N.: Numerical Methods for Solving Convection-Diffusion. URSS, Moscow (1999)
26. Thomée, V.: Galerkin Finite Element Methods for Parabolic Problems, *Springer Series in Computational Mathematics*, vol. 25, second edn. Springer-Verlag, Berlin (2006)
27. Vabishchevich, P.N.: Decoupling schemes for predicting compressible fluid flows. Comput. & Fluids **171**, 94–102 (2018)
28. Von Neumann, J., Richtmyer, R.D.: A method for the numerical calculation of hydrodynamic shocks. J. Appl. Phys. **21**, 232–237 (1950)
29. Wesseling, P.: Principles of Computational Fluid Dynamics, *Springer Series in Computational Mathematics*, vol. 29. Springer-Verlag, Berlin (2001)
30. Zienkiewicz, O.C., Taylor, R.L., Nithiarasu, P.: The Finite Element Method for Fluid Dynamics, seventh edn. Elsevier/Butterworth Heinemann, Amsterdam (2014)